Heavy precipitation events in a warmer climate: results from CMIP5 models

Enrico Scoccimarro[1,2]*
Silvio Gualdi[1,2]
Alessio Bellucci[2]
Matteo Zampieri[2]
Antonio Navarra[1,2]

[1]Istituto Nazionale di Geofisica e Vulcanologia (INGV), Bologna, Italy

[2]Centro Euro-Mediterraneo sui Cambiamenti Climatici (CMCC), Bologna, Italy

Journal of Climate, DOI: 10.1175/JCLI-D-12-00850.1 - Accepted May-16-2013

Corresponding authors addresses:

-Enrico Scoccimarro, Centro Euro-Mediterraneo sui Cambiamenti Climatici (CMCC), V.le A.Moro 44, 40127 Bologna, Italy. E-mail: enrico.scoccimarro@bo.ingv.it

-Silvio Gualdi, Centro Euro-Mediterraneo sui Cambiamenti Climatici (CMCC), V.le A.Moro 44, 40127 Bologna, Italy. E-mail: silvio.gualdi@bo.ingv.it

-Alessio Bellucci, Centro Euro-Mediterraneo sui Cambiamenti Climatici (CMCC), V.le A.Moro 44, 40127 Bologna, Italy. E-mail: alessio.bellucci@cmcc.it

-Matteo Zampieri, Centro Euro-Mediterraneo sui Cambiamenti Climatici (CMCC), V.le A.Moro 44, 40127 Bologna, Italy. E-mail: matteo.zampieri@cmcc.it

-Antonio Navarra, Centro Euro-Mediterraneo sui Cambiamenti Climatici (CMCC), V.le A.Moro 44, 40127 Bologna, Italy. E-mail: antonio.navarra@cmcc.it

Abstract:

In this work the authors investigate possible changes in the distribution of heavy precipitation events under a warmer climate, using the results of a set of 20 climate models taking part in the Coupled Model Intercomparison Project phase 5 effort (CMIP5). Future changes are evaluated as the difference between the last four decades of the 21st and the 20th Century assuming the Representative Concentration Pathway RCP8.5 scenario. As a measure of the width of the right tail of the precipitation distribution, we use the difference between the 99th and the 90th percentiles. Despite a slight tendency to underestimate the observed heavy precipitation, the considered CMIP5 models well represent the observed patterns in terms of the ensemble average, during both summer and winter seasons for the 1997-2005 period. Future changes in average precipitation are consistent with previous findings based on CMIP3 models. CMIP5 models show a projected increase for the end of the twenty-first century of the width of the right tail of the precipitation distribution, particularly pronounced over India, South East Asia, Indonesia and Central Africa during boreal summer, as well as over South America and southern Africa during boreal winter.

38

1. Introduction

39

40 Changes in the frequency and intensity of extreme events can affect human health directly through
41 heat waves and cold spells and indirectly through floods or pollution episodes (Zwiers and Kharin
42 1998, Parry et al. 2007, Peterson et al. 2008). The associated societal implications make an accurate
43 simulation of extremes by climate models a particularly relevant issue. In the past years many
44 studies have been undertaken to analyze intense precipitation events using coupled and uncoupled
45 General Circulation Models (GCMs) (Wetherald and Manabe 1999, Kharin and Zwiers 2000,
46 Hegerl et al. 2004, Kharin et al. 2007, Hegerl et al., 2007, Kiktev et al. 2007, Carril et al. 2008, Min
47 et al. 2009, Seager et al. 2012), investigating their capability in detecting changes of extreme
48 precipitation, when analyzing twentieth and twenty-first century climate simulations. Model
49 projections indicate intensification of extreme precipitation in a warming climate leading to wet
50 areas getting wetter and dry areas getting drier (Chou et al 2009). The availability of a new set of
51 climate simulations for the twenty-first century, carried out with state of the art coupled GCMs
52 produced for the fifth Coupled Model Intercomparison Project (CMIP5, Meehl and Bony, 2012),
53 gives us the possibility to investigate future changes in intense precipitation following one of the
54 Representative Concentration Pathways (RCPs) considered as illustrative of potential future
55 scenarios. The present analysis is performed following the RCP8.5 scenario, the one with the
56 highest rate of increase in greenhouse gas concentrations within the new set of RCPs. The main aim
57 of this work is to inspect changes in the shape of the right tail of the precipitation events distribution
58 under warmer conditions, comparing the last part of the twenty-first century with the last part of
59 the twentieth century, as simulated by a set of CMIP5 climate models. The paper is organized as
60 follows. Section 2 describes the data and provides an overview of the methodology used, Section 3
61 presents the results of the analyses, and Section 4 summarizes the main points of the study and
62 concludes the paper.

63

64 2. Data and Methodology

65 2.1. *Reference data*

66 For this analysis we use daily precipitation fields from a subset of the CMIP5 multimodel
67 ensemble, consisting of simulations of the twenty and twenty-first century climate performed with
68 20 coupled ocean-atmosphere climate models (see table 1). CMIP5 simulations are conducted in
69 support of the fifth assessment report of the Intergovernmental Panel on Climate Change (IPCC-
70 AR5). The horizontal resolution of the atmospheric component of the considered models ranges
71 from about 0.75 to about 3.5 degrees with a median of 1.7 degrees. Two periods are analysed: the
72 period 1966-2005 (hereafter PRESENT), corresponding to the last part of the 'historical' CMIP5
73 simulation and the period 2061-2100 (hereafter FUTURE), run under the high-end RCP8.5 scenario
74 (Riahi et al. 2011, Taylor et al. 2012). The 'historical' simulation is performed forcing CMIP5
75 models with observed concentrations of greenhouse gasses, aerosols, ozone and solar irradiance,
76 starting from an arbitrary point of a quasi-equilibrium control run. The RCP8.5 scenario follows a
77 rising radiative forcing pathway leading to 8.5 W/m^2 in 2100.

78 For this analysis we make use of daily precipitation fields. The capability of the CMIP5
79 models to simulate the present climate in terms of heavy precipitation events has been assessed
80 using daily data from the Global Precipitation Climatology Project (GPCP, Bolvin et al., 2009), of
81 the period 1997-2005 (hereafter PRES). On the suitability of the use of GPCP data for investigating
82 intense precipitation see Shiu et al. 2012 and Liu et al. 2009. In the rest of the paper, for the sake of
83 simplicity we will refer to the GPCP data as 'observations'. In this work we aim to assess potential
84 changes in precipitation extremes that might have a societal impact, thus we mainly focus on
85 precipitation over land.

86

86

87 *2.2. Methodology*

88 To investigate how CMIP5 models represent intense precipitation compared to observations,
89 we computed the 90th and 99th percentiles (hereafter 90p and 99p) over the distribution of
90 precipitation obtained by aggregating daily precipitation values, belonging to the investigated
91 period, over each single grid point. Furthermore, in our analysis, we want also to assess how heavy
92 rainfall, defined as daily events with a precipitation amount greater than the 90p, might change in
93 intensity. To this aim, we use the difference between the 99p and 90p, where the former is
94 representative of very intense precipitation and the latter is the threshold used to define an event as
95 heavy rainfall. This metric has been defined, separately for PRESENT and FUTURE climates, to
96 quantify the width of the right tail of the precipitation distribution. In the present analysis, the
97 impact of the non stationarity of precipitation time series associated with the high-hand RCP8.5
98 scenario has been found non significant. Percentiles are computed for each model, on the
99 corresponding original spatial grid. Individual model results have been then interpolated onto the
100 GPCP regular grid to allow the multi-model averaging.

101 For abbreviation purposes, we will refer to 'future changes' to indicate changes between the
102 FUTURE (2061-2100) and the PRESENT (1966-2005) periods.

103 # 3. Results

104 Previous assessments (Kharin et al. 2007, O'Gorman and Schneider 2009) have shown that
105 climate models provide a realistic representation of present-day heavy precipitation in the extra-
106 tropics, but uncertainties in heavy precipitation in the Tropics are very large. The 90p and 99p
107 (Figure 1 shows the zonal average of the 99th percentile computed at each grid point) are
108 consistently simulated at middle and high latitudes by CMIP5 models, but they tend to
109 underestimate these indices in the Tropics, especially in the northern summer, but also at high

latitudes in the Northern Hemisphere during northern winter and Southern Hemisphere during northern summer (Figure 1). This tendency is noticeably less pronounced when only models with a horizontal resolution finer than 1.5 degrees are considered (about 50% of the CMIP5 models used in this analysis, see table 1), but the dispersion around the mean does not change (not shown). The observed spatially average amount of rainfall, associated with heavy precipitation events (>90p, computed for each grid cell) over land during the PRES period, is about 55% of the total precipitation in both winter and summer seasons (circles in Figure 2, first panel). The corresponding estimate provided by CMIP5 models amounts to less than 45% (squares in Figure 2, first panel) during the PRESENT period in summer and winter. A closer agreement between CMIP5 models and observations is found when we focus on the rainfall associated with very intense precipitation events (>99p): the corresponding amount of water in the observations is about 12% (circles in Figure 2, second panel), which is within the uncertainty range of the CMIP5 models. The model results shown in figure 2 do not change considering the 1966-2005 or the shorter 1997-2005 period. Very similar results have been found using the globally averaged amount of rainfall including precipitation over the sea (not shown). During the FUTURE period, the CMIP5 box plots are shifted upward by 2-5%, suggesting a slight increase in the amount of rainfall associated with heavy precipitation, over land, in a warmer climate.

The width of the range of values attributable to observed (Figure 3, left panels) heavy precipitation events, as represented by the 99p-90p metric, is reasonably well reproduced by the CMIP5 ensemble average (Figure 3, right panels). The model ensemble mean properly captures observed spatial patterns, despite a general tendency to underestimate 99p-90p over most of the Tropics and, especially, in the Amazonian basin, equatorial Africa, Mediterranean basin and northern Australia in DJF. In JJA, the models appear to overestimate the intense events in the north-eastern part of the North American and Asian continent and Hymalayan region. The locations where the intense precipitation appears to be overestimated, correspond with the areas where the models precipitation has a positive bias (not shown). Future changes in climatological precipitation

patterns (Figure 4 left panels) are overall coherent with previous findings (Giorgi and Bi, 2009) obtained using CMIP3 (the previous phase of the Coupled Model Intercomparison Project) models. During boreal winter a general increase in precipitation over land is found, except for Central America and South America. During boreal summer, a general increase of precipitation over land at latitudes higher than 55^{o}N is found and a strong decrease over Southern Europe, up to 60%, is made apparent (red pattern in figure 4, bottom-left panel). A less intense decrease in the average precipitation appears also over Western North America, Central America, equatorial South America and Western Africa around 15^{o} North (figure 4, left panels). Future changes in 90p (Figure 4, central panels) follow the described changes in average precipitation. The usage of 99p-90p gives the possibility to better investigate changes in the right tail of the distribution of precipitation events, especially over regions where both 90p and 99p increase/decrease. In fact, despite the very similar patterns found in future changes of climatological precipitation and 90p (Figure 4, left and central panels respectively), the 99p-90p changes, pertaining to heavy precipitation events (Figure 4, right panels), look different: in the FUTURE period the 99p-90p metric increases worldwide, even over regions where average precipitation and 90p values show a decrease (red patterns in Figure 4). This is the case of southeast Europe during summer, where the width of the right tail of the distribution increases, even if nearly the entire precipitation distribution becomes dryer (i.e., decreases in total, 90p, and 99p precipitation). Over some regions the 99p-90p increase reaches 180% of the PRESENT period precipitation value (blue patterns in Figure 4, right panels), amounting to about 8 mm/d over land between 30^{o}S and the Equator, during boreal winter and involving all continents. These intense positive patterns move northward between 5^{o}S and 15^{o}N during boreal summer, covering Africa and South America, reaching maximum values of 10 mm/d over India, southern China and Indochina. A future increase in the width of the right tail of the precipitation events distribution, greater than 5 mm/d, is also evident along the Eastern coast of Asia, up to Siberia, during the boreal summer. The largest increases in 99p-90p, of greater than 12 mm/d, are found in the Indonesian region in both seasons.. The described long term tendencies for

the 99p-90p metric were also found in a separate analysis performed grouping rainfall data over 26 regions (Figure 6) selected following the IPCC special report on extreme events (IPCC, 2012). We separately assessed the 99p-90p changes for the entire domain and for land-points only. It is found (not shown) that for both DJF and JJA, the vast majority of the selected regions shows a positive increment of the 99p-90p index. No significant differences are found with or without the inclusion of the ocean portion of each regional domain. This positive tendency is more pronounced for the rightmost part of the rainfall distribution, compared with the leftmost part, as highlighted in figure 7 where changes in moderate heavy, very intense and extreme events (75^{th} ,90^{th} ,99^{th}, 99.9^{th} percentiles, respectively) in the FUTURE period with respect to the PRESENT period are shown.

4. Discussion and Conclusions

In this paper we apply the difference between 99^{th} and 90^{th} percentile of the daily precipitation resulting from a set of twenty CMIP5 simulations, with the aim of quantifying potential changes in the width of the right tail of precipitation distribution, thus to the range of values attributable to a heavy (greater than 90p) precipitation event.

Precipitation intensity seems to increase more than mean precipitation under a warmer climate, confirming previous findings (Trenberth et al. 2003; Meehl et al, 2005; Chou et al. 2009). These changes are consistent with a greater moisture-holding capacity of the warmer air contributing to greater moisture convergence (Tebaldi et al., 2006) and with the Clausius–Clapeyron dependence which is relevant for heavy precipitation events (Giorgi et al., 2011), which are able to empty the atmospheric moisture column (Allen and Ingram 2002; Allan and Soden 2008). It is in fact well known that increases in atmospheric water vapour content are generally associated with increases in heavy precipitation in a warmer climate (e.g., Pall et al. 2007, O'Gorman and Schneider 2009). The width of the right tail of the precipitation event distribution increases almost everywhere (Figure 4 right panels), independently of the direction in which the distribution evolves in a warmer climate, suggesting more heavy precipitation events especially over the Tropics during summer. The

187 increased availability of water in a warmer climate, is confirmed by the water vapour content
188 (WCONT), vertically integrated through the atmospheric column. The regions affected by strong
189 stretching of the right tail of precipitation event distribution in the future (blue patterns in figure 4,
190 right panels) correspond to strong increased availability of water vapour content in the atmospheric
191 column (blue patterns in Figure 5, right panels).

192 To a first approximation, if one considers no changes in precipitation efficiency (here defined as the
193 ratio of total precipitation to total available moisture), we would link the increased width of the
194 right tail of FUTURE precipitation distribution to the increased availability of WCONT. Regional
195 changes in the atmospheric circulation patterns (Hertig et al. 2013) might also alter the statistics of
196 the heavy rain events. However a conclusive disentangling of the causes underlying the detected
197 changes in the precipitation distribution is beyond the purpose of this work. In summary, despite the
198 fact that model projections of future changes in heavy precipitation events in response to global
199 warming might be underpredicted (Allan and Soden, 2008), a picture of a world with intensifying
200 heavy precipitation events over the majority of land seems confirmed by CMIP5 model projections
201 for the end of the twenty-first century, at least following a future scenario with a continuous rise in
202 radiative forcing during the twenty-first century. This implies increasing risks for natural and
203 human systems that are sensitive to wet extremes (Kunkel et al. 1999; Giorgi et al., 2011).

204

205 ***Acknowledgments***. The research leading to these results has received funding from the Italian
206 Ministry of Education, University and Research and the Italian Ministry of Environment, Land and
207 Sea under the GEMINA project. We also acknowledge the World Climate Research Programme's
208 Working Group on Coupled Modelling, which is responsible for CMIP, and we thank the climate
209 modelling groups for producing and making available their model output. For CMIP the U.S.
210 Department of Energy's Program for Climate Model Diagnosis and Intercomparison provided

211 coordinating support and led development of software infrastructure in partnership with the Global
212 Organization for Earth System Science Portals.
213

References

Allen, M. R., and W. J. Ingram, 2002: Constraints on the future changes in climate and the hydrological cycle. *Nature*, 419, 224–232.

Allan R.P. and Soden, B.J, 2008: Atmospheric Warming and the Amplification of Precipitation Extremes. *Science*. (321): 1481-1484.

Bolvin, D. T., R. F. Adler, G. J. Huffman, E. J. Nelkin, J. P. Poutiainen, 2009: Comparison of GPCP monthly and daily precipitation estimates with high-latitude gauge observations. *J. Appl. Meteor. Climatol*., 48, 1843-1857.

Carril A., S. Gualdi, A. Cherchi, A. Navarra, 2008: Heatwaves in Europe: Areas of homogeneous variability and links with the regional to large-scale atmospheric and SSTs anomalies. *Clim. Dyn*. 30: 77-98.

Chou, C., J. D. Neelin, C. Chen, and J. Tu, 2009: Evaluating the 'rich-get-richer' mechanism in tropical precipitation change under global warming. *J. Climate*, 22, 1982–2005.

Giorgi, F. and X. Bi, 2009: Time of emergence (TOE) of GHG-forced precipitation change hot-spots, *Geophys. Res. Lett*., 36, L06709, doi:10.1029/2009GL037593.

Giorgi, F., E.-S. Im, E. Coppola, N. S. Diffenbaugh, X. J. Gao, L. Mariotti, Y. Shi, 2011: Higher Hydroclimatic Intensity with Global Warming. *J. Climate*, 24, 5309–5324.

O'Gorman, P.A. & T. Schneider, 2009) The physical basis for increases in precipitation extremes in simulations of 21st-century climate change. *Proceedings of the National Academy of Sciences* 106, 14773-14777

Hegerl, G.C., F.W. Zwiers, P.A. Stott and V.V. Kharin, 2004: Detectability of anthropogenic changes in annual temperature and precipitation extremes. *J. Clim.* 17,3683–3700.

Hegerl, G.C. et al. Climate Change 2007, 2007: The Physical Science Basis (eds Solomon, S. et al.) 663–745 (*Cambridge Univ. Press*).

Hertig E., S. Seubert, A. Paxian, G. Vogt, H. Paeth, J. Jacobeit, 2013: Changes of total versus extreme precipitation and dry periods until the end of the twenty-first century: statistical assessments for the Mediterranean area. *Theoretical and Applied Climatology*, 111 (1-2), pg. 1-20.

Kharin, V.V., F.W. Zwiers, 2000: Changes in the extremes in an ensemble of transient climate simulations with a coupled atmosphere–ocean GCM. *J. Climate* 13, 3760–3788.

Kharin V.V., F.W. Zwiers, X. Zhang, G.C. Hegerl, 2007: Changes in temperature and precipitation extremes in the IPCC ensemble of global coupled model simulations. *J. Climate* 20, 1419 –1444.

Kiktev,D., J. Caesar, L.V. Alexander, H. Shiogama and M.Collier, 2007: Comparison of observed and multimodeled trends in annual extremes of temperature and precipitation. *Geophys. Res. Lett*. 34, L10702, doi:10.1029/2007GL029539.

261 Kunkel, K. E., Pielke R. Jr. and Changnon, S. A., 1999: Temporal fluctuations in weather and
262 climate extremes that cause economic and human health impacts: A review. *Bull. Am. Met. Soc*.
263 80,1077–1098.
264
265 IPCC, 2012: Managing the Risks of Extreme Events and Disasters to Advance Climate Change
266 Adaptation. A Special Report of Working Groups I and II of the Intergovernmental Panel on
267 Climate Change [Field, C.B., V. Barros, T.F. Stocker, D. Qin, D.J. Dokken, K.L. Ebi, M.D.
268 Mastrandrea, K.J. Mach, G.-K. Plattner, S.K. Allen, M. Tignor, and P.M. Midgley (eds.)].
269 Cambridge University Press, Cambridge, UK, and New York, NY, USA, 582 pp.
270
271 Liu, S. C., C. Fu, C.-J. Shiu, J.-P. Chen, and F. Wu, 2009: Temperature dependence of global
272 precipitation extremes, *Geophys. Res. Lett.,* 36, L17702, doi:10.1029/ 2009GL040218.
273
274 Meehl, G. A., J. M. Arblaster, and C. Tebaldi, 2005: Understanding future patterns of increased
275 precipitation intensity in climate model simulations. *Geophys. Res. Lett.*, 32, L18719, doi:10.1029/
276 2005GL023680.
277 Meehl, G.A. and S. Bony, 2012: Introduction to CMIP5. WCRP Coupled Model Intercomparison
278 Project – Phase 5: Special Issue of the CLIVAR Exchanges Newsletter, No. 56, Vol. 15, No. 2
279
280 Min,S.-K., X.B. Zhang, F.W. Zwiers, P. Friederichs and A. Hense, 2009: Signal detectability in
281 extreme precipitation changes assessed from twentieth century climate simulations. *Clim. Dyn.* 32,
282 95–111.
283
284 Pall P., Allen M.R., Stone D.A., 2007: Testing the Clausius-Clapeyron constraint on changes in
285 extreme precipitation under CO2 warming. *Clim Dyn* 28:351–363.
286
287 Parry, M. L., O.F. Canziani,, J.P. Palutikof, P.J. van der Linden and C.E. Hanson (eds Solomon, S.
288 et al.) Climate Change 2007, 2007: Impacts, Adaptation and Vulnerability (*Cambridge Univ.*
289 *Press*).
290
291 Peterson, T. C. et al., 2008: Weather and Climate Extremes in a Changing Climate. Regions of
292 Focus: North America, Hawaii, Caribbean, and U.S. Pacific Islands (eds Karl, T. R. et al.) 11–34.
293 Synthesis and Assessment Product 3.3, US Climate Change Science Program, Washington DC.
294
295 Riahi K, S Rao, V Krey, C Cho, V Chirkov, G Fischer, G Kindermann, N Nakicenovic, P Rafaj,
296 2011: RCP 8.5—A scenario of comparatively high greenhouse gas emissions. *Climatic Change*.
297 109:33-57. DOI 10.1007/s10584-011-0149-y.
298
299 Seager, R., N. Naik, L. Vogel, 2012: Does Global Warming Cause Intensified Interannual
300 Hydroclimate Variability? *J. Climate*, 25, 3355–3372.
301
302 Shiu, C-J, S. C. Liu, C. Fu, A. Dai, Y. Sun., 2012: How much do precipitation extremes change in a
303 warming climate?. *Geophys. Res. Lett.* 39:17 DOI:10.1029/2012GL052762.
304
305 Taylor, K.E., R.J. Stouffer, G.A. Meehl, 2012: An Overview of CMIP5 and the experiment design."
306 *Bull. Amer. Meteor. Soc*., 93, 485-498, doi:10.1175/BAMS-D-11-00094.1.
307
308 Tebaldi C., K. Hayhoe, M.J. ARBLASTER and G. A. MEEHL, 2006: Going to the Extremes
309 An Intercomparison of Model-Simulated Historical and Future Changes in Extreme Events.
310 Climatic Change 79: 185–211 DOI: 10.1007/s10584-006-9051-4.
311

312 Trenberth, K. E., A. Dai, R. Rasmussen, and D. Parsons, 2003: The changing character of
313 precipitation. Bull. Amer. Meteor. Soc., 84, 1205–1217.
314
315
316 Wetherhald, R.T., S. Manabe, 1999: Detectability of summer dryness caused by greenhouse
317 warming. *Clim. Change* 43, 495 – 511.
318
319 Zwiers, F.W., V.V. Kharin, 1998: Changes in the extremes of the climate simulated by CCC GCM2
320 under CO2 doubling. *J. Climate* 11, 2200–2222.
321
322

322

Model name	Lat x Lon (degrees)	Institute (Institude ID)
BNU-ESM	2.8 x 2.8	College of Global Change and Earth System Science, Beijing Normal University (GCESS)
CCSM4	**0.9 x 1.5**	National Center for Atmospheric Research (NCAR)
CMCC-CESM	3.7 x 3.7	Centro Euro-Mediterraneo sui Cambiamenti Climatici (CMCC)
CMCC-CMS	1.9 x 1.9	Centro Euro-Mediterraneo sui Cambiamenti Climatici (CMCC)
CMCC-CM	**0.8 x 0.8**	Centro Euro-Mediterraneo sui Cambiamenti Climatici (CMCC)
CNRM-CM5	**1.4 x 1.4**	Centre National de Recherches Meteorologiques / Centre Europeen de Recherche et Formation Avancees en Calcul Scientifique (CNRM- CERFACS)
CSIRO-Mk3-6-0	1.9 x 1.9	Commonwealth Scientific and Industrial Research Organization in collaboration with Queensland Climate Change Centre of Excellence (CSIRO-QCCCE)
CanESM2	2.8 x 2.8	Canadian Centre for Climate Modelling and Analysis (CCCMA)
FGOALS-s2	1.6 x 2.8	LASG, Institute of Atmospheric Physics, Chinese Academy of Sciences (LASG-IAP)
GFDL-CM3	2.0 x 2.5	NOAA Geophysical Fluid Dynamics Laboratory (NOAA GFDL)
GFDL-ESM2G	2.0 x 2.5	NOAA Geophysical Fluid Dynamics Laboratory (NOAA GFDL)
GFDL-ESM2M	2.0 x 2.5	NOAA Geophysical Fluid Dynamics Laboratory (NOAA GFDL)
HadGEM2-CC	**1.2 x 1.8**	Met Office Hadley Centre (MOHC)
HadGEM2-ES	**1.2 x 1.8**	Met Office Hadley Centre (MOHC)
INM-CM4	**1.5 x 2.0**	Institute for Numerical Mathematics (INM)
IPSL-CM5A-MR	**1.2 x 2.5**	IPSL-CM5A-LR Institut Pierre-Simon Laplace (IPSL)
MIROC5	**1.4 x 1.4**	Atmosphere and Ocean Research Institute (The University of Tokyo), National Institute for Environmental Studies, and Japan Agency for Marine-Earth Science and Technology (MIROC)
MPI-ESM-MR	1.9 x 1.9	Max Planck Institute for Meteorology (MPI-M)
MRI-CGCM3	**1.1 x 1.1**	Meteorological Research Institute (MRI)
NorESM1-M	1.8 x 2.5	Norwegian Climate Centre (NCC)

323 Tab 1. CMIP5 models involved in this study. Bold values in the second column indicate horizontal

324 resolution finer than 1.5^{o}.

325

326

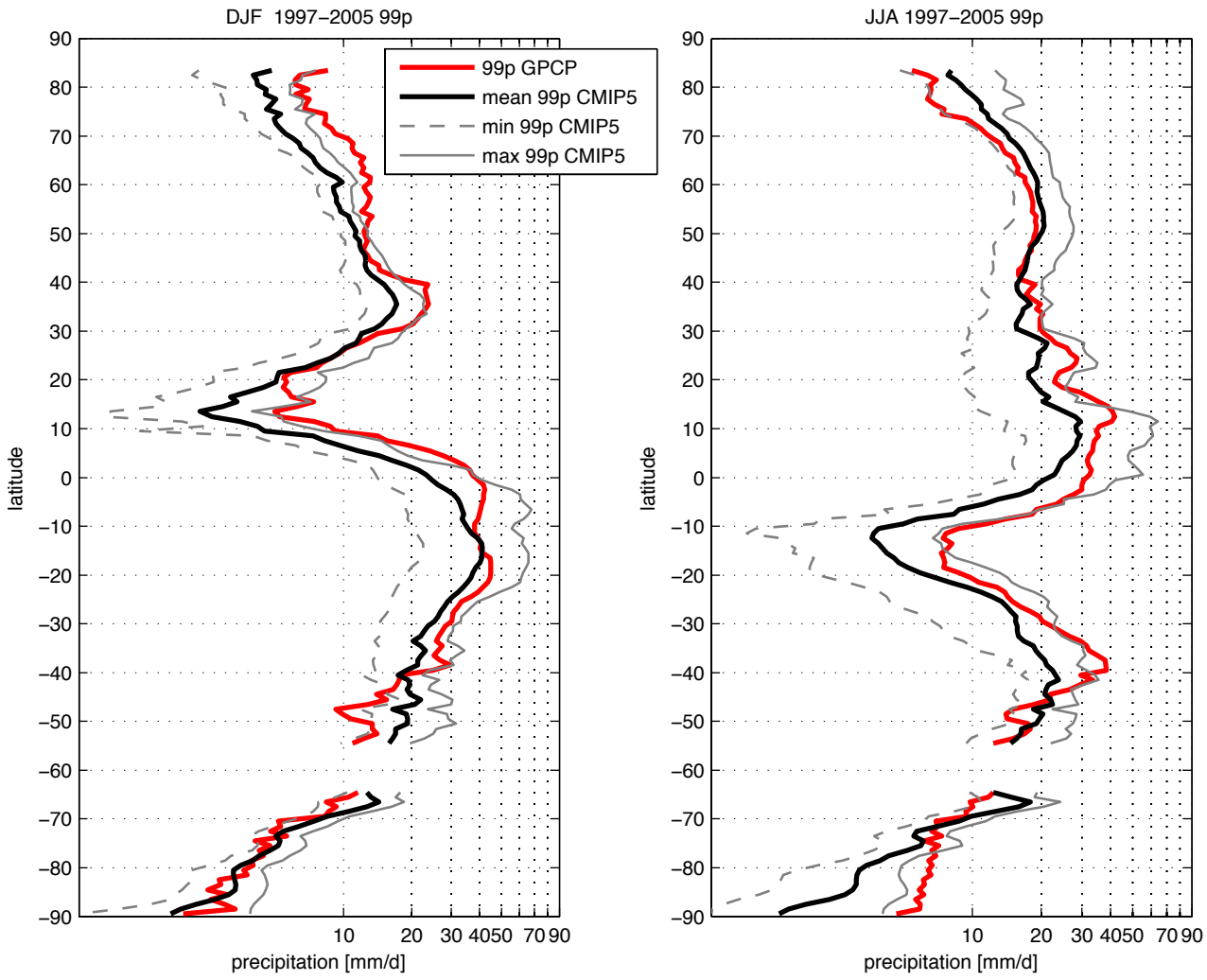

FIG. 1. 99th percentile (99p) of daily precipitation for the period 1997-2005 in CMIP5 historical simulations (black lines) and observations (red lines), as a function of latitude, over land. Gray lines represent the minimum (dashed) and maximum (solid) 99th percentiles at each latitude, within the 20 CMIP5 models considered. A logarithmic scale has been adopted for the x axis. Units are [mm/d].

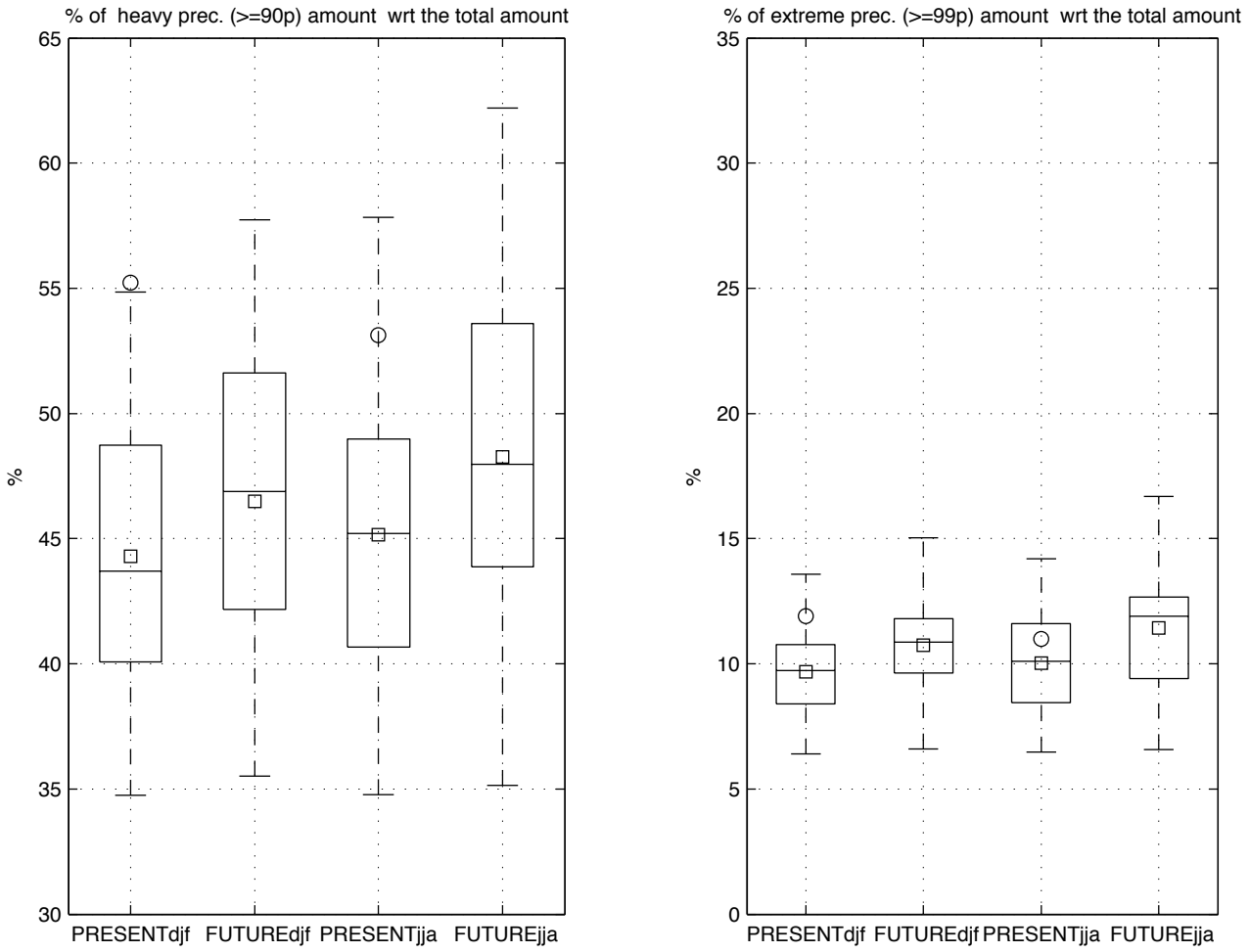

FIG. 2. Box plots of the fraction of precipitation associated with heavy events (>90p, left panel) and very intense events (>99p, right panel) with respect to the total precipitation amount. The box plots represent the distribution of the 20 CMIP5 models. In each panel, the first two box plots represent the boreal winter season (DJF) and the last two box plots represent the boreal summer season (JJA) under PRESENT (1966-2005) and FUTURE (2061-2100) periods. The percentage of water associated with heavy/very intense events (y-axis) is computed over land at global scale. In each box plot, the box represents the interquartile range (IQR) and contains 50% of the data; the upper edge of the box represents the 75th percentile (upper quartile, UQ), while the lower edge is the 25th percentile (lower quartile, LQ). The horizontal lines within the box are the median, the squares are the mean. The vertical dashed lines indicate the range of the non-outliers (outliers are values that are either larger than UQ + 1.5 · IQR or smaller than LQ -1.5 · IQR). Circles represent the observed value over the PRES (1997-2005) period.

346

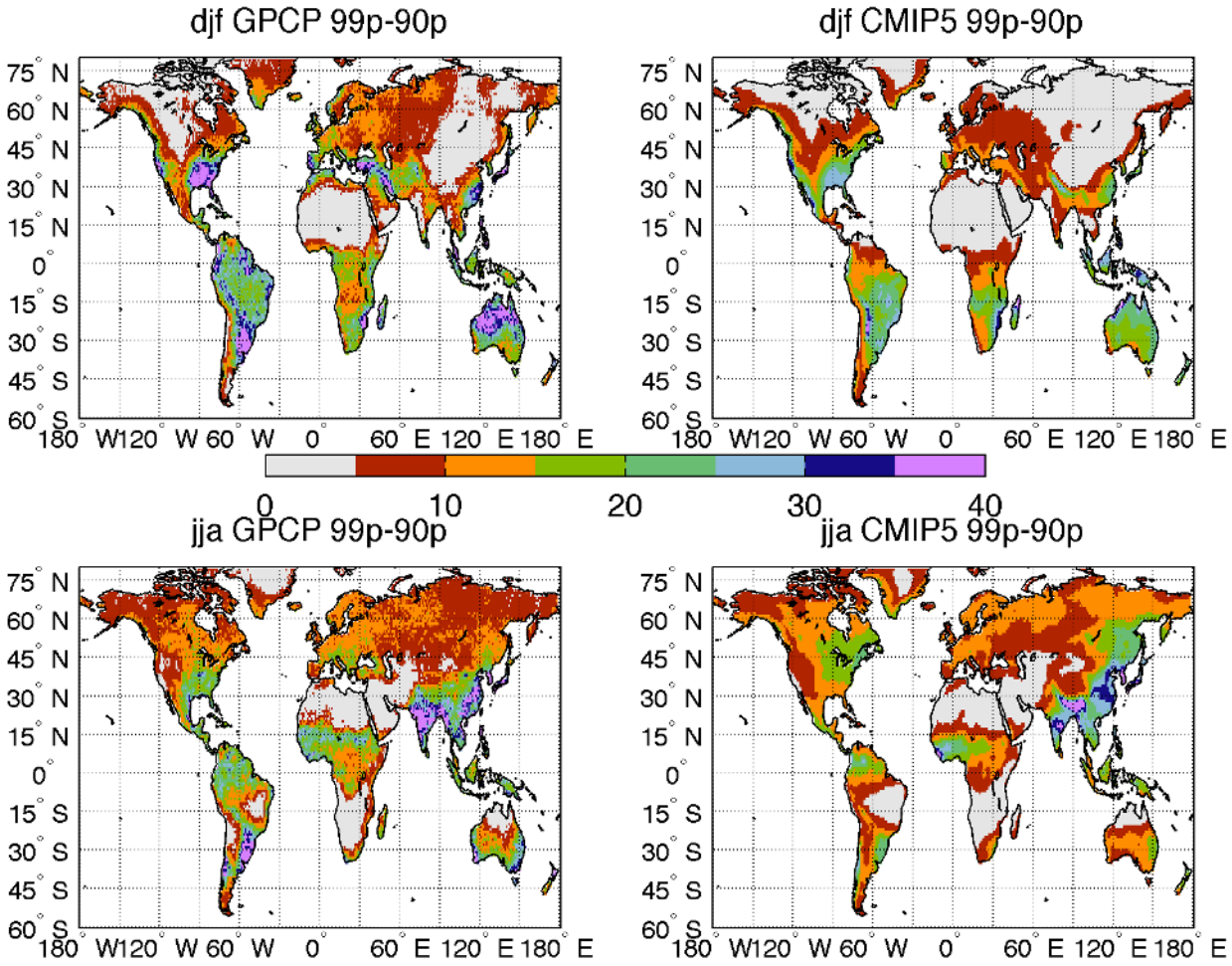

347

348 FIG. 3. Measure of the right tail of the precipitation events distribution, represented as 99p-90p
349 during the period 1997-2005 as obtained by the observations (left panels) and CMIP5 (average over
350 the 20 models, right panels). Upper panels refer to boreal winter and lower panels refer to boreal
351 summer. Units are [mm/d].

352

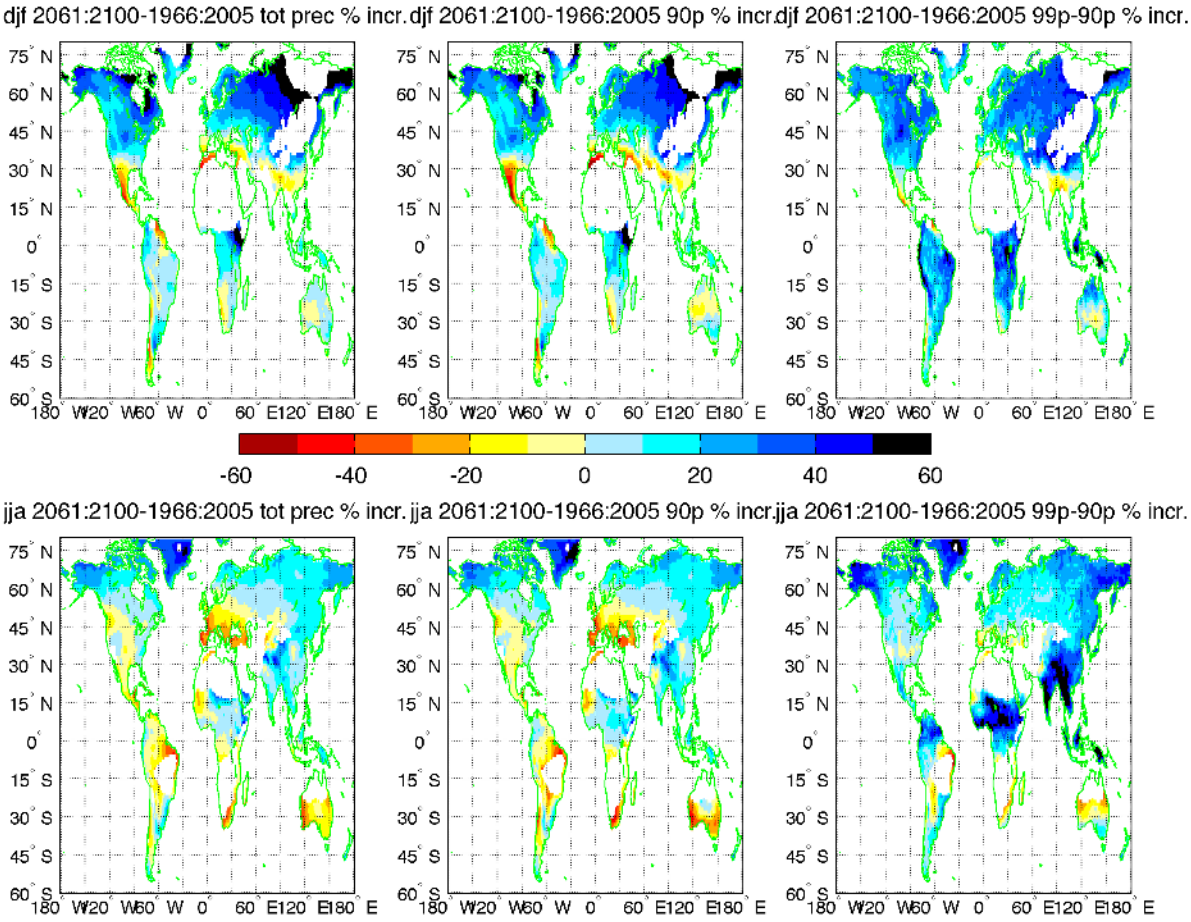

352

353 FIG. 4. Future changes (2061-2100 – 1966-2005) in average precipitation (left panels), 90th
354 percentile of precipitation (90p, central panels) and width of the right tail of the precipitation events
355 distribution (99p-90p, right panels) following the RCP8.5 CMIP5 scenario, as averaged over the
356 CMIP5 models. Upper panels refer to boreal winter and lower panels refer to boreal summer. Units
357 are [%]. White patterns over land indicate regions with seasonal precipitation lower than 0.5 mm/d.

358

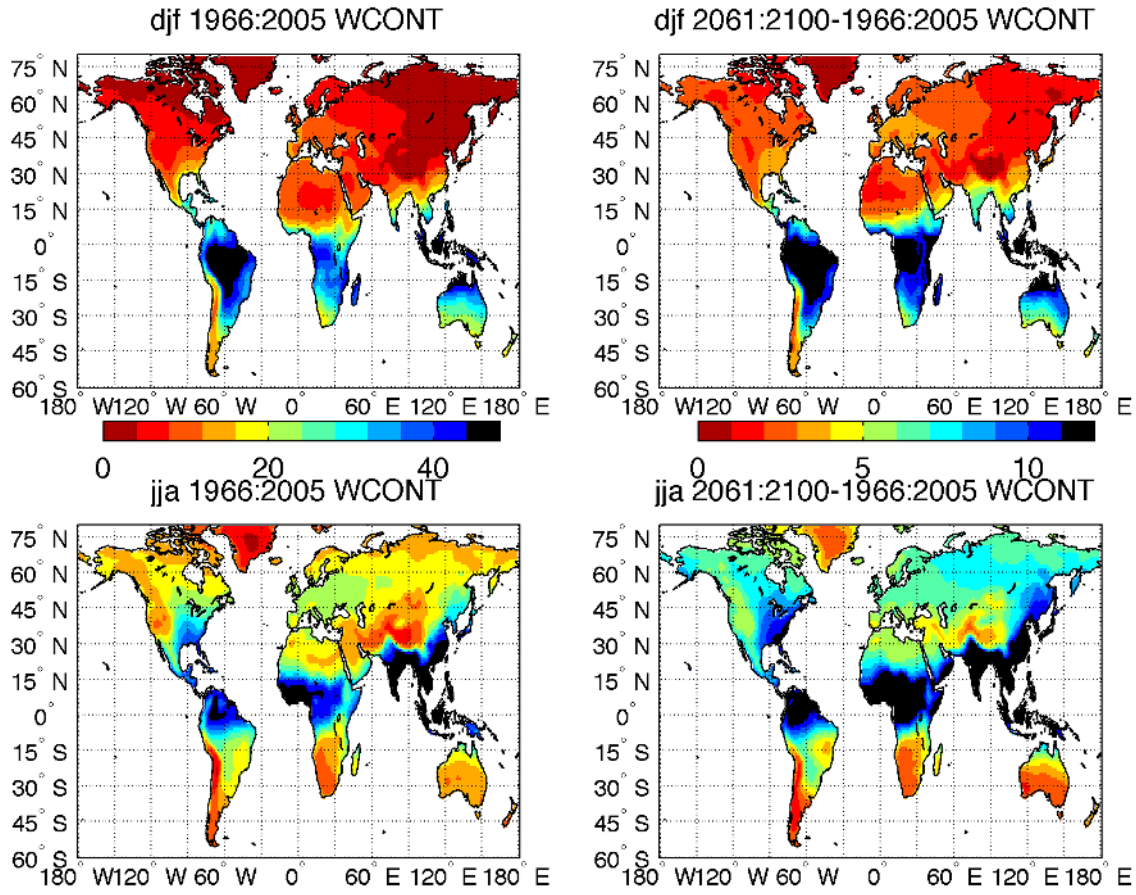

359

360 FIG. 5. Water vapour content (WCONT), vertically integrated through the atmospheric column,
361 during the 1966-2005 period (left panels) and increase in 2061-2100 wrt 1966-2005 as averaged
362 over the CMIP5 models. Upper panels refer to boreal winter and lower panel refer to boreal
363 summer. Units are [Kg/m^2].

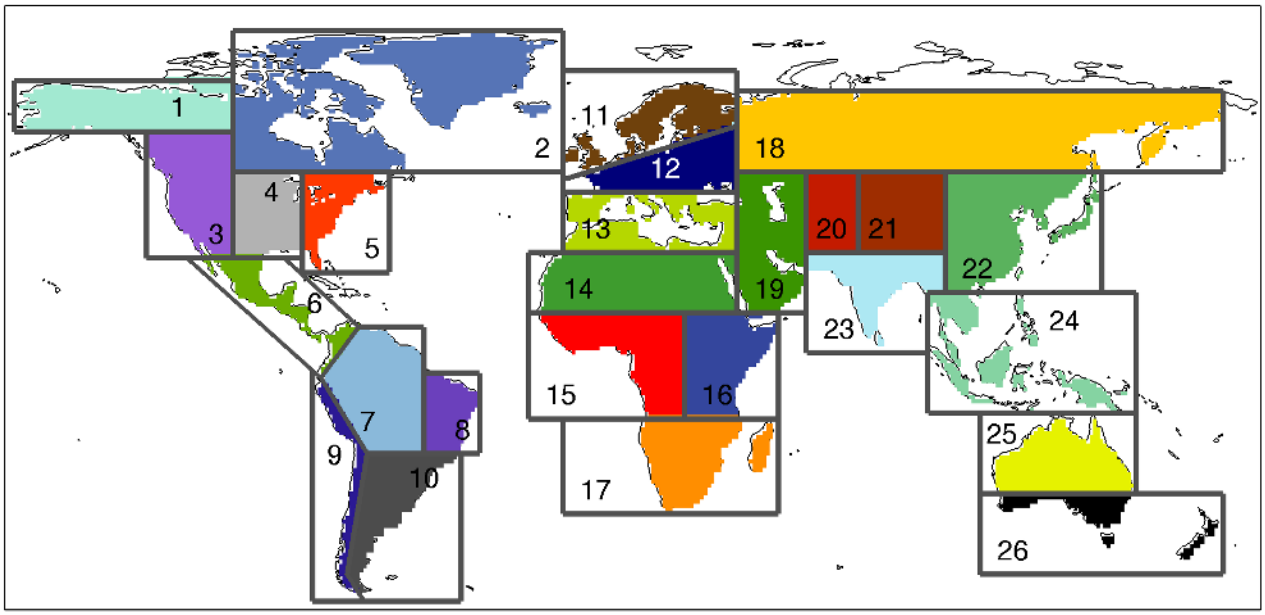

364

365 FIG. 6. Regions defined to group rainfall data.

366

367

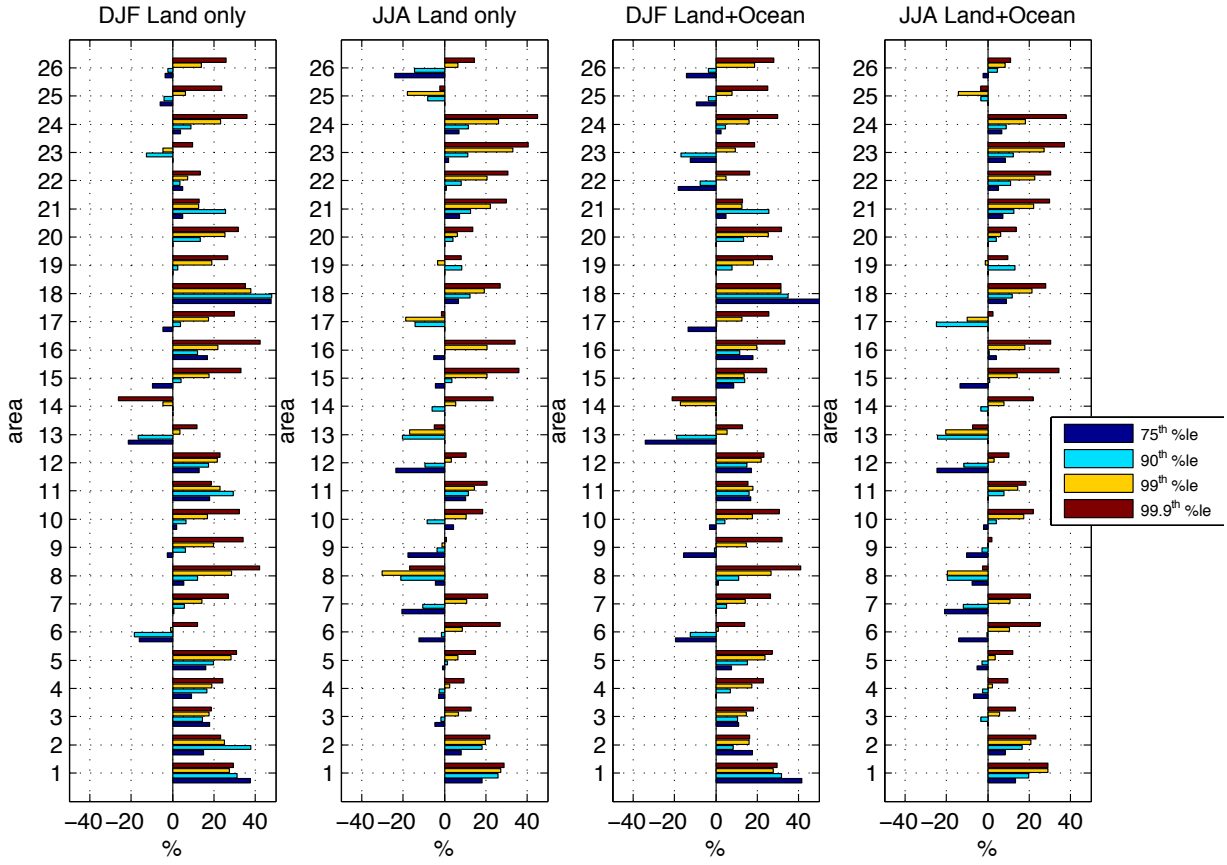

367

368 FIG. 7. Future changes (2061-2100 wrt 1966-2005) of moderate (75th percentile, blue), heavy (90th
369 percentile, light blue), very intense (99th percentile, yellow) and extreme (99.9th percentile, red)
370 events computed over 26 areas (defined in figure 6). The first two panels refer to land only (colors
371 in figure 6). The last two panels refer to land and ocean. Boreal winter is shown in the 1st and 3rd
372 panels. Boreal summer is shown in the 2nd and 4th panels. Units are [%].

373

374